Aerosol Optical Characteristics in the Yellow Sand Events Observed in May, 1982 at Nagasaki-Part I Observations

By Masayuki Tanaka, Masataka Shiobara[1]

Teruyuki Nakajima and Maki Yamano[2]

Upper Atmosphere Research Laboratory, Tohoku University, Sendai 980, Japan

and

Kimio Arao

Faculty of Education, Nagasaki University, Nagasaki 852, Japan
(Manuscript received 24 October 1988, in revised form 14 February 1989)

Abstract

Optical thicknesses and volume spectra of aerosols were retrieved from spectral extinction and aureole measurements for the yellow sand events observed during 4–8 May 1982 at Nagasaki, Japan. The results showed a dominance of large particles of several micron radius and a reduction of submicron particles. The mode radius of the column volume spectrum obtained with the aureolemeter was larger than two microns during the yellow sand events. The aerosol optical thickness at a wavelength of 0.5μm and the Ångström's exponent α took values of 0.5–1.0 and 0.1–0.5 in contrast with their normal values of 0.2–0.8 and 0.8–1.5, respectively. Trajectory analyses from the synoptic charts as well as the elemental composition, the number density and the scattering cross section of aerosols supported consistently the prevalence of the continental air mass associated with the frontal activity during the yellow sand events.

1. Introduction

A large amount of yellow sand particles is uplifted in the Chinese Continent by frontal activities in spring season and transported to Japan and the North Pacific region. They are one of the main sedimentation materials in the North Pacific Ocean floor (Duce *et al.*, 1980) and constitute a considerable fraction of soil derived aerosols which amount to 40–50 % of the total aerosols over the Japan Islands in April and May (Kadowaki, 1979; Tanaka *et al.*, 1983b). Dust storm events occur over the Eastern Asian deserts as frequently as about one third of the time and these events are responsible for a notable aerosol source with strength about 0.5 ton/sec (Junge, 1979; Shaw, 1980). Particularly, heavy dust storms apparently observed in Japan are familiarly called Kosa in Japanese, and in recent years, have come to be quantitatively observed by ground-based soundings (Iwasaka *et al.*, 1982; Arao and Ishizaka, 1986; Kai *et al.*, 1988). Sometimes the dust travels even to the Hawaiian Islands (Shaw, 1980; Darzi and Winchester, 1982; Braaten and Cahill, 1986). Those observations show that yellow sand particles contribute significantly to the atmospheric turbidity over a large area of the North Pacific region in spring season, though frequency of the observable yellow sand event at a fixed location is as small as about 5 days/year even at Nagasaki, the most south-western part of the Japan Islands (Arao *et al.*, 1979).

In spite of the important role of yellow sand particles as noted above, investigation of optical characteristics of the particles is quite insufficient as compared with that for Saharan dust storms (*e.g.* Carlson and Caverly, 1977; Tomasi *et al.*, 1979; Carlson and Benjamin, 1980; Kondratyev *et al.*, 1981; Welch *et al.*, 1981). In order to elucidate the optical characteristics of aerosols in yellow sand events, we carried out measurements of the solar radiation and aerosols using several instruments for the period of 22 April to 12 May, 1982. In this and the following papers (Nakajima *et al.*, 1989) we de-

[1]Present affiliation: Meteorological Research Institute, Tsukuba 305, Japan.

[2]Present address: 2-9-10, Nagao, Tama-ku, Kawasaki 214, Japan.

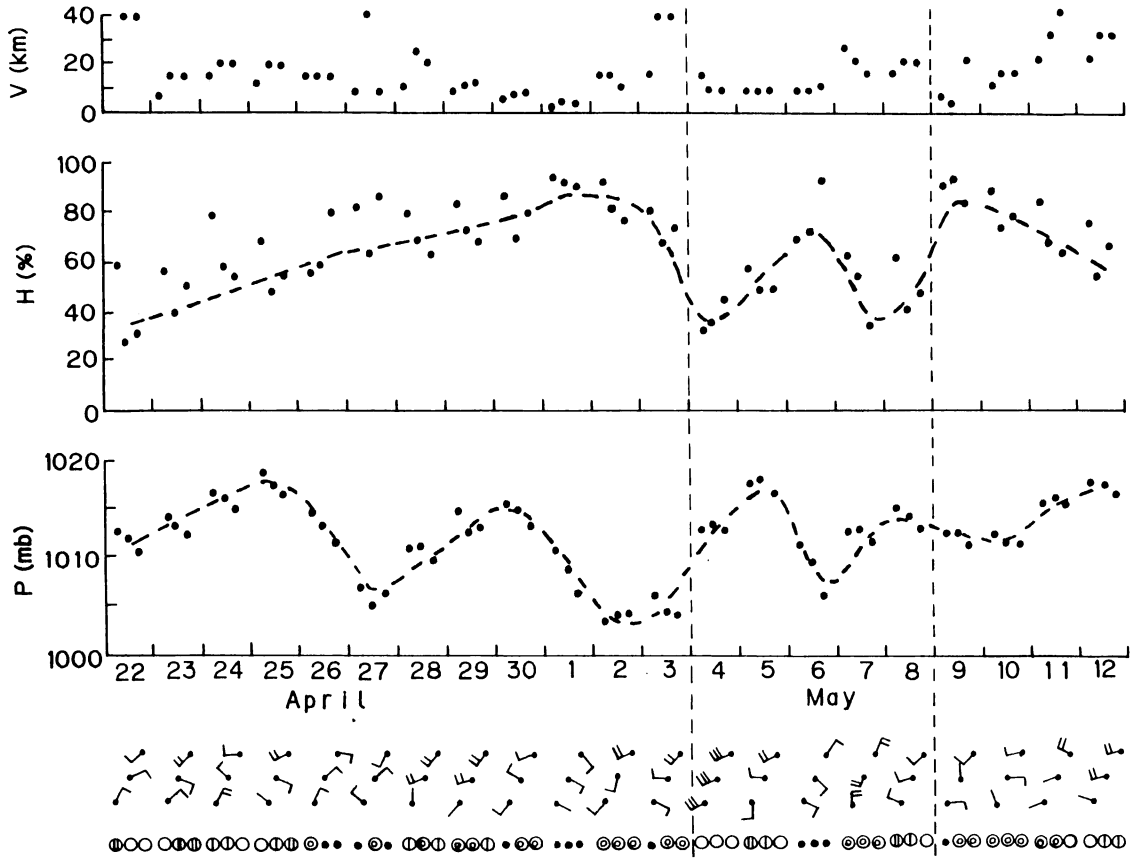

Fig. 1. Time series of the visibility (V), relative humidity (H), pressure (P), wind vector and weather condition during the observation period.

scribe the result of the measurements and discuss the features of the aerosol optical characteristics in the events.

2. Measurements

Solar radiation and aerosol properties were measured at the campus of Nagasaki University (32° 47'N, 129° 52'E, 12 m above MSL) near the center of Nagasaki city, which is located in a valley of an isthmus between Ohmura Bay and East China Sea, during the period from 22 April to 12 May, 1982. The system for the measurement and observed quantities were similar to those of Nakajima *et al.* (1986). We presently introduced an improved aureolemeter and a compact polar nephelometer, which were simultaneously used with an optical particle counter (OPC, RION KC-01), a nuclepore filter sampler and an eight-stage Andersen sampler. Data of the diffuse radiative flux were not available in the present case. The instruments were set up on the top of a building of Nagasaki University (25 m high).

Direct-solar and circumsolar radiations were measured by the aureolemeter at wavelengths of λ = 0.369, 0.500, 0.675, 0.776 and 0.862 μm. The minimum observable scattering angle of the aureolemeter is about 2°. The measured data were used to retrieve the size distribution of aerosols by applying a multispectral inversion method of Nakajima *et al.* (1983). Detailed specification and calibration method of the aureolemeter were described in Tanaka *et al.* (1986). For the optical counter (OPC) measurement, the air was sampled with a rate of 0.54 *l*/min through a vinyl tube of 8 mm diameter and 2 m long. The dust in the air was sampled on nuclepore filters with the pore size of 0.08 μm. We carried out the PIXE (Proton Induced X-ray Emission) analysis of the nuclepore filters using a 3 MeV proton beam of the Cyclotron Radioisotope Center of Tohoku University. The Andersen sampler was used to measure time-mean values of the aerosol mass spectrum near the ground surface during 4–6 May when the yellow sand event was most significant in the observation period. By the compact polar nephelometer, several phase matrix elements were measured at wavelength of 0.633 μm for scattering angles between 7° and 170°. Detailed description of the measurement using the polar nephelometer will be given in Nakajima *et al.* (1989).

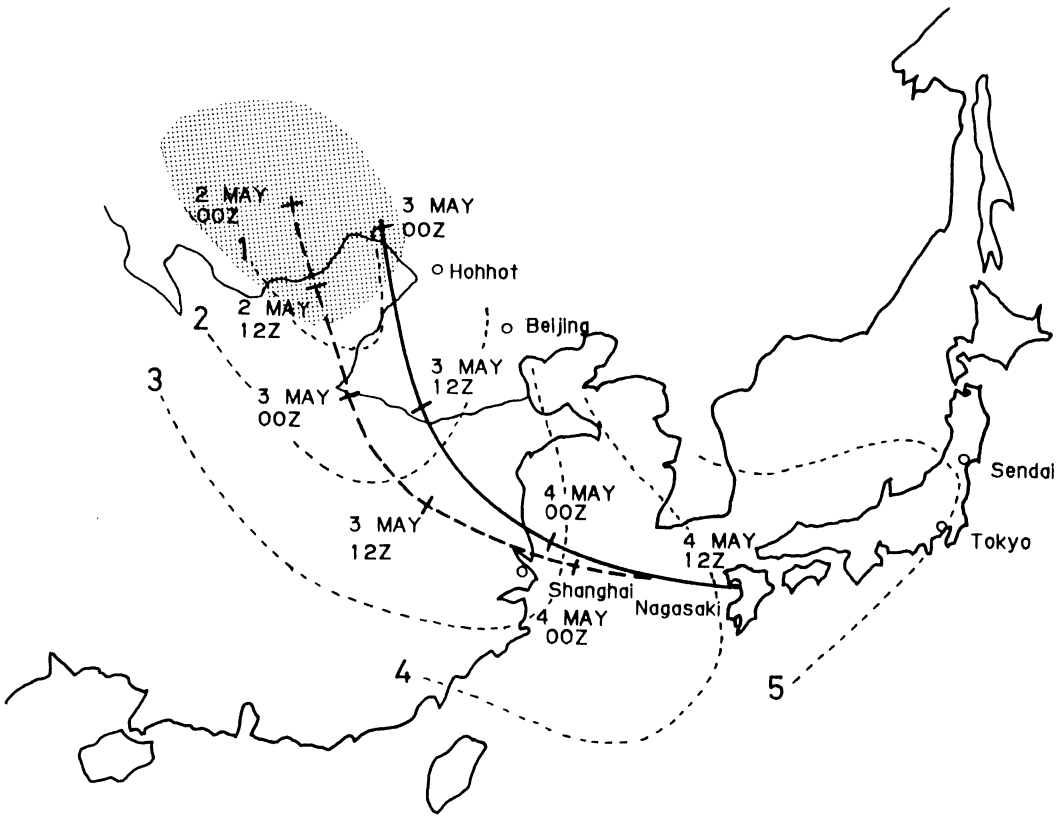

Fig. 2. Fronts (dashed lines) and trajectories at 700 mb (solid line) and 850 mb (broken line) for the air mass laden with yellow sand particles generated by the storms on 30 April–2 May. The hatched area is the region of the sand storms recorded on the map.

3. Yellow sand events and transportation of dust particles

a. Meteorological condition and map analysis

Figure 1 shows time series of meteorological elements provided by Nagasaki Marine Observatory. After a low passed on 21 April, the observation site was covered by a travelling high during 22–25 April. The weather at the site became rainy on 27 April by the activity of a weak low travelling through Shanghai and the southern offshore of Japan. Although the observation site was again covered by a high after the day, a trough in the upper layer persisted and the atmosphere was in an unstable condition during 28–30 April. Relative humidity was gradually increasing in this period. With deepening of the trough, a low over Northern China grew and reached the eastern offshore of Hokkaido on 4 May. After the cold front associated with the low passed, a significant yellow sand event was observed all over Japan. At Nagasaki, the low passed on 2 May and the yellow sand event was observed on 4 May. Intrusion of the continental air mass was observed by reduction of atmospheric visibility down to 8 km and the relative humidity to 30 %. The trough in the upper layer persisted after 4 May, and another low was travelling over Japan on 6 May. With this activity of the low, a yellow sand event was recorded in China and Korea, while no event was recorded in Japan. After 6 May, the weather of the observation site was unstable through the activity of a front on the southern offshore of Japan.

Positions of fronts and trajectories of the air mass laden with yellow sand particles were obtained for the yellow sand event of 4–5 May from the analysis of synoptic charts of 00Z and 12Z as shown in Fig. 2. During the period from 30 April to 4 May, dust storms were observed every day around the Badain-jaran and Gobi Deserts. Backward trajectory analyses from several locations in Japan showed that trajectories of 850 mb level, as well as 700 mb level, were consistent with the surface record of yellow sand events over China and Japan. Figure 2 indicates that yellow sand particles were uplifted around those deserts and transported southward over Central China and deflected eastward toward Japan. Since the isobaric trajectory analysis adopted here is insufficient to discuss the origin and the altitude of transportation precisely, we roughly conclude that the origin was in an arid region around the middle course of the Yellow River (Huang-he) and the altitude of transportation was in the lower troposphere.

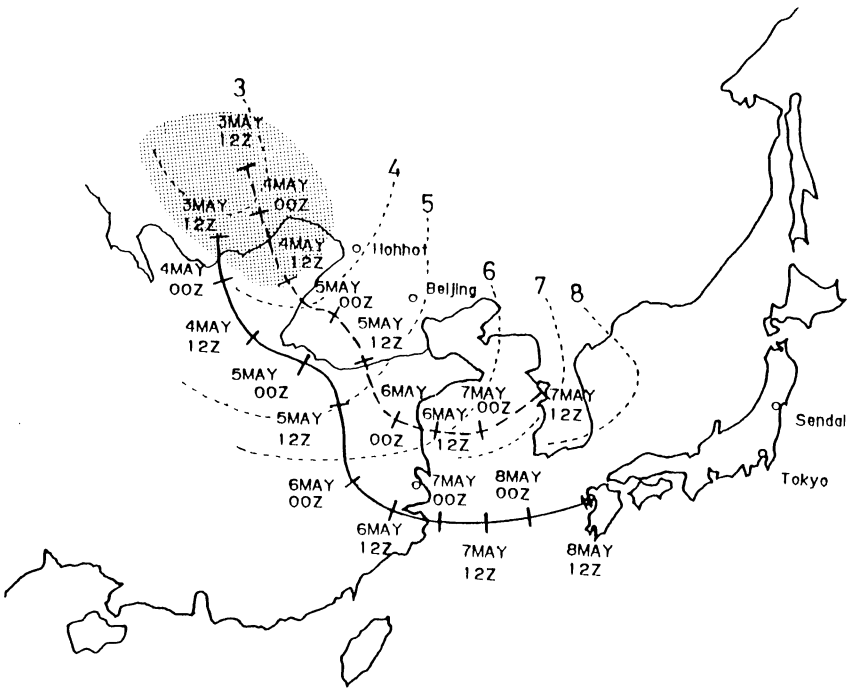

Fig. 3. Same as in Fig. 2 but for 850 mb trajectories backward from Nagasaki (solid line) and Seoul (dashed line) corresponding to the sand storm generated on 3–4 May.

This altitude is consistent with the fact that several lidar measurements showed a layered structure with a principal peak around 2 km (Iwasaka *et al.*, 1982; Kobayashi *et al.*, 1985). On the other hand this altitude is a little lower than the mean level of transportation of about 4 km reported by Arao *et al.* (1979) and Kai *et al.* (1988).

As for the weak yellow sand event of 7–8 May which was observed over Korea, the origin was also in the arid region around the middle course of the Yellow River as shown in Fig. 3. The backward trajectory suggests that the air mass over Nagasaki came by way of a periphery of the source region and, therefore, that no large amount of sand particles was transported to Japan. Furthermore the moving speed of the air mass in this case was lower than the event of 4–5 May, so that a significant portion of yellow sand particles would fall out during the transportation. The air mass over Nagasaki on 8 May is considered to include a small amount of aged yellow sand particles, although no event was recorded by Nagasaki Marine Observatory.

b. Characteristics of the air mass

Yellow sand events are judged more objectively by an elemental analysis of dust particles sampled on nuclepore filters. Figure 4 shows mass fractions of principal elements of aerosols sampled at the observation site and of sand sample collected near Lanzhou in the middle course of the Yellow River. For the elemental analysis, we selected iron,calcium,

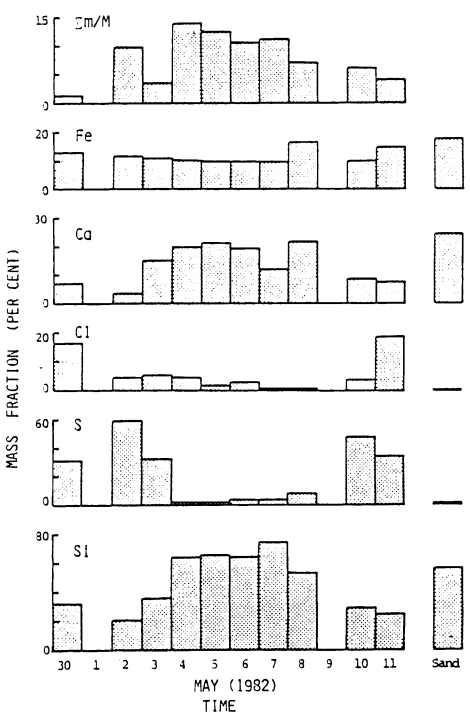

Fig. 4. Elemental fractions of aerosols in the observation period and of sand sample collected near Lanzhou, PRC. Total mass fraction of the principal elements (Σ_m/M) is shown at the top and the fractions of the respective elements (*Fe, Ca, Cl, S* and *Si*) relative to their total mass (Σ_m) are shown below in per cent.

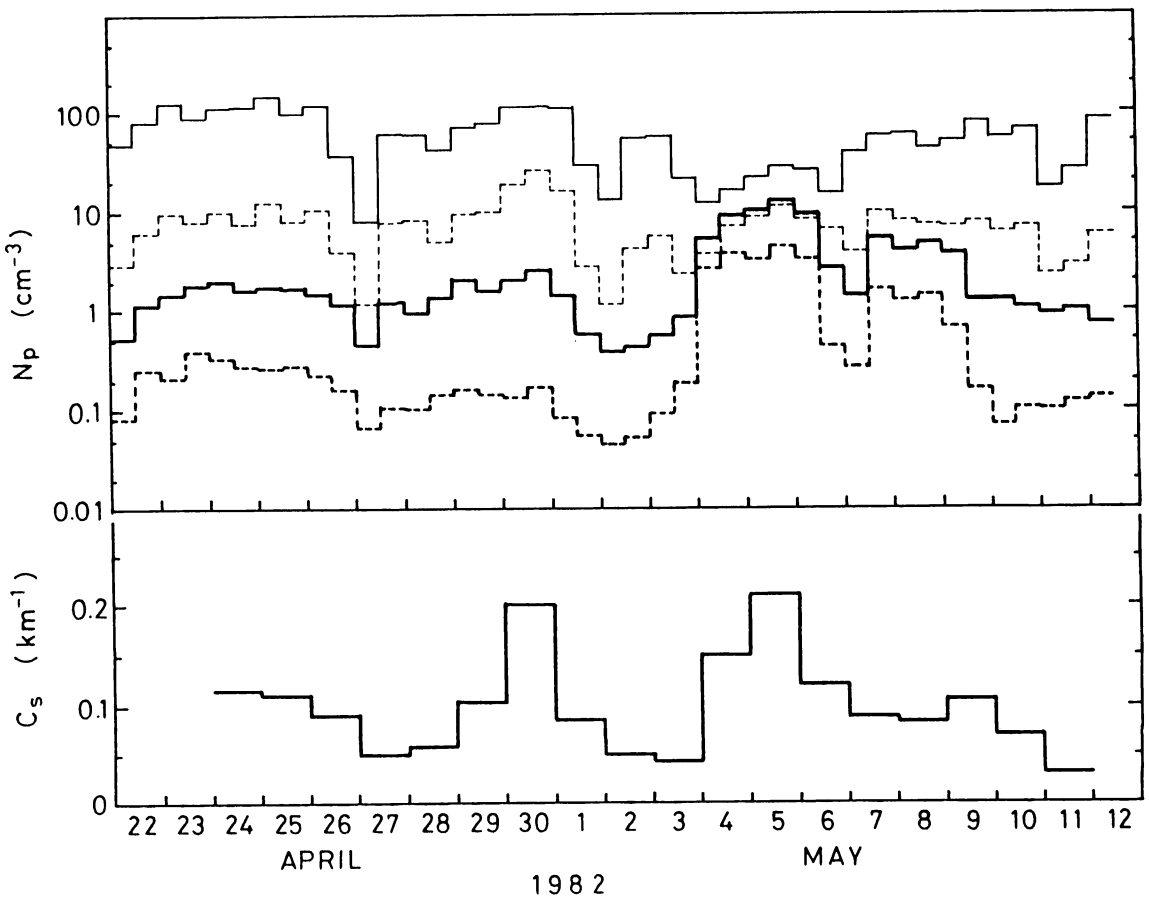

Fig. 5. Time series of the particle number density (N_p) for $0.15 \leq r \leq 0.25$ μm(thin solid line), $0.25 \leq r \leq 0.5$ μm (thin dashed line), $0.5 \leq r \leq 1.0$ μm (thick solid line) and $1.0 \leq r \leq 2.5$ μm (thick dashed line), and the scattering cross section (C_s) at wavelength of 0.633 μm.

chlorine, sulfur and silicon in this study. Dominance of silicon and calcium and lack of sulfur and chlorine were characteristic for aerosols in the yellow sand events during the period of 4–8 May and the elemental fractions were similar to those of the sand sample from Lanzhou. The fraction of silicon to the total mass (*Si* times $\Sigma m/M$ in Fig. 4) was about 7.7 % in the yellow sand events and 2.7 % in the normal conditions at the site. According to Kadowaki (1979), the fractions of silicon and aluminum are well correlated with each other, and thus, they are good indicators of aerosols of soil origin. Our values are consistent with his result, *i.e.*, the fraction was about 6.1 % in spring season and 2 to 3 % in other seasons in Nagoya. Although the iron can be a characteristic element of the dust sand particles (Kondratyev *et al.*, 1974), it was not a good indicator of yellow sand particles in our case. According to Winchester *et al.* (1981), the weight ratio of calcium to iron (*Ca/Fe*) was 2.0 for coarse aerosols and 1.0 for fine aerosols in a rural area in North China in spring time. Braaten and Cahill (1986) also reported values around 1.0 for this weight ratio for Asian dust particles transported to Hawaii. In our case the *Ca/Fe* weight ratio increased significantly during the yellow sand events from 0.6 to 2.0. The *Si/Fe* ratio also increased during the events from 2.3 to 6.4, although the value of 6.4 was higher than those reported in the other references, *i.e.* 3.1 (the sand sample in this study), 4.0 (Winchester *et al.*) and 3.4 (Braaten and Cahill). Since the fraction of each element depends significantly on the particle size, more detailed comparisons will be necessary to understand the nature of these quantitative differences.

Figure 5 shows a time series of the aerosol number density measured by the OPC and the scattering cross section obtained by integrating the phase function measured by the polar nephelometer. In the observation period, two peaks of the scattering cross section were observed on 30 April and 5 May. On 30 April the number density of all particles with radii smaller than 1.0 μm increased, while on 5 May the number density of particles with radii larger than 0.5 μm increased but that of smaller particles decreased. The former peak of the scattering cross section corresponds to a misty atmospheric condition of 30 April when a maritime high prevailed and the

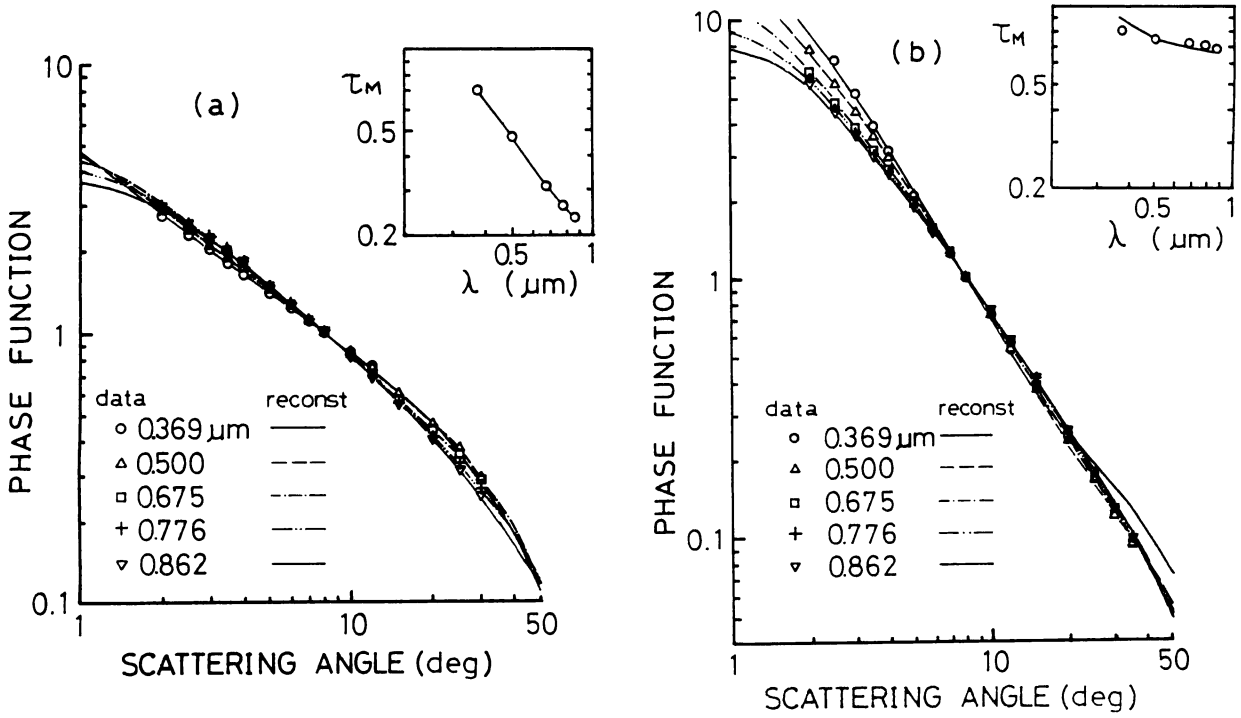

Fig. 6. Forward part of the phase function and the optical thickness in the normal condition (a: 24 April, 1982) and in the yellow sand event (b: 4 May, 1982). Symbols show the data obtained by the aureolemeter and lines the reconstructed values using the retrieved volume spectra shown in Fig. 8.

relative humidity reached 80 % as shown in Fig. 1. Small fractions of insoluble materials such as *Fe*, *Ca* and *Si* to the total mass and relative increases of the fractions of *Cl* and *S* shown in Fig. 4 also suggest a significant growth of hygroscopic aerosols by absorbing water vapor. On the other hand the latter peak corresponds to the maximum stage of the yellow sand events. Figure 5 shows three minima of the particle number density on 27 April, 2 and 6–7 May. The agreement of appearance of the minima with those of the surface pressure in Fig.1 shows that aerosols were sometimes removed by passage of lows in the observation period.

Hereafter we divide the whole period of the observation into three stages, *i.e.* the period prior to 3 May, 4–8 May, and after 9 May. We classify the middle stage as the yellow sand event and the other two as the normal conditions.

4. Optical characteristics of aerosols

a. Feature of the radiative data

Investigations of the aerosol optical properties have shown that submicron aerosols are responsible for large part of light scattering in the normal conditions of a suburban area in Japan (Tanaka *et al.*, 1983a; Nakajima *et al.*, 1986). The atmospheric circumstance was very different in the yellow sand events. Figure 6 shows the spectral optical thicknesses and the forward part of aerosol phase function retrieved from the data of the aureolemeter by using an iterative scheme of Nakajima *et al.* (1983) to subtract the multiple scattering. The forward scattering was significantly enhanced and wavelength dependence of the optical thickness was reduced as compared with those in the normal conditions. These features of the light scattering and extinction were attributed primarily to the large fraction of particles as large as several microns similar to those of the Saharan dust (Prodi and Tomasi, 1983).

Since the forward part of the phase function was not largely depending on wavelengths for both the normal conditions and the yellow sand events (see Fig. 6), a power law volume spectrum was expected to provide a good approximation. According to Nakajima *et al.* (1983), the power p of the power law volume spectrum

$$dV/dlnr = Cr^{4-p}$$

where r is the particle radius, can be estimated from the wavelength dependence of the optical thickness for small particles and from the scattering angle dependence of the forward part of the phase function for large particles. It was found that the value of p for small particles was somewhat dependent on the assumed maximum particle radius, so that we used the following revised relation for the optical thickness with the maximum particle radius $r_{max} = 10\mu$m assumed in our analysis:

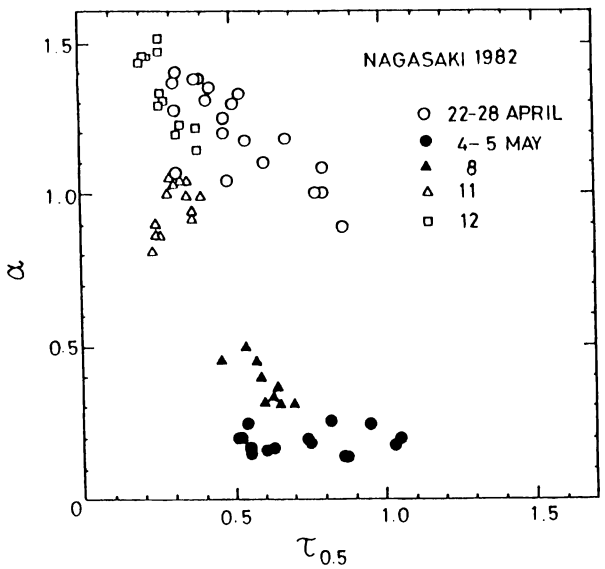

Fig. 7. Relationship between α and $\tau_{0.5}$ for the period of 22–28 April (open circles), 4–5 May (closed circles), 8 May (closed triangles), 11 May (open triangles) and 12 May (open rectangles).

$$p = 2.76 + 1.35\alpha$$

where α is the power of the Ångström's approximation of the spectral optical thickness of aerosols as

$$\tau = \tau_{0.5}(0.5/\lambda)^{\alpha}$$

with λ in μm. On the other hand, a relationship between the power p and the slope of the forward part of phase function, $dlnP(\Theta)/dln\Theta$, was given by Nakajima *et al.* (1983) as

$$dlnP(\Theta)/dln\Theta = -3.97\exp(-0.0509p^{2.5})$$

where $P(\Theta)$ is the phase function at the scattering angle Θ.

In Fig. 6, we have p= 4.58 and 3.98 for the data of 24 April while p = 2.98 and 3.25 for the data of 4 May, respectively for small and large particles. For the normal condition the large difference of p-values between small and large particles shows a bimodal feature of the volume spectrum, while the small difference of p-values for the case of the yellow sand events shows that the size distribution of the yellow sand particles was nearly approximated by a power law function.

Figure 7 shows the parameter α as a function of the aerosol optical thickness $\tau_{0.5}$ at λ = 0.5μm. Open symbols show the data in the normal conditions, while closed symbols correspond to the data in the yellow sand events. It is found that the optical thickness increased slightly in the yellow sand events and reached a value from 0.5 to 1.0, which is larger than the values of 0.2–0.8 for the normal condition. The value around 0.6 was also estimated by Takayama and Takashima (1986) for the yellow sand events in 1984 from a satellite data analysis. The values of α were 0.8–1.5 and 0.2–0.5 for the normal conditions and the yellow sand events, respectively. Such a range of α for the normal conditions is quite consistent with other previous results (*e.g.* Ångström, 1964; Yamamoto and Tanaka, 1969; Tanaka *et al.*, 1983a). The rather discontinuous decrease of α is a characteristic feature of the yellow sand events corresponding to the great enhancement of large dust particles (Figs. 6 and 9). It was also found that the α value was inversely proportional to $\tau_{0.5}$ for the normal conditions especially in the pre-event stage. This means that the atmospheric turbidity increases with an increase of large particles in contrast to the general trend of background aerosols in the clean air mass presented by Shaw (1977). This contradiction will be explained by the difference of aerosol origins and history. In a clean air condition, generation and aging of aerosols are important during spreading from a remote source. The exponent α will mainly increase with an increase of the number of accumulation mode aerosols especially for a low turbidity (Kaufman and Fraser, 1983). On the other hand, growth of hygroscopic aerosols with an increase of the relative humidity (Takamura *et al.*, 1984; Takeda *et al.*, 1986) and removing of background aerosols with frontal activities noted in Figs. 1 and 2 would be important in such a condition as the pre-event stage.

b. Retrieval of the column volume spectrum

Since the extinction and forward scattering are rather independent of the nonsphericity of the particle (Asano and Sato, 1980), a reliable column volume spectrum will be obtained by the inversion of combined data of the optical thickness and forward part of the column phase function. Figure 8 shows the volume spectra which were retrieved by the inversion method of Nakajima *et al.* (1983) using the data shown in Fig. 6. The volume spectra were retrieved for particle radii between about 0.1 and 8 μm. If no phase function data are available, the retrievals are limited to submicron particles as shown by triangles in Fig. 8. The optical thickness and phase function reconstructed using these volume spectra are shown by lines in Fig. 6. Good agreements with the measured values indicate that the retrieved volume spectra were adequate to explain the observed data. The p-values for small and large particles estimated respectively from the optical thickness and the phase function are also shown by broken lines in Fig. 8. These examples show that the simple parameterization indicated in Sec.4a is consistent with the fundamental shape of the retrieved column volume spectrum.

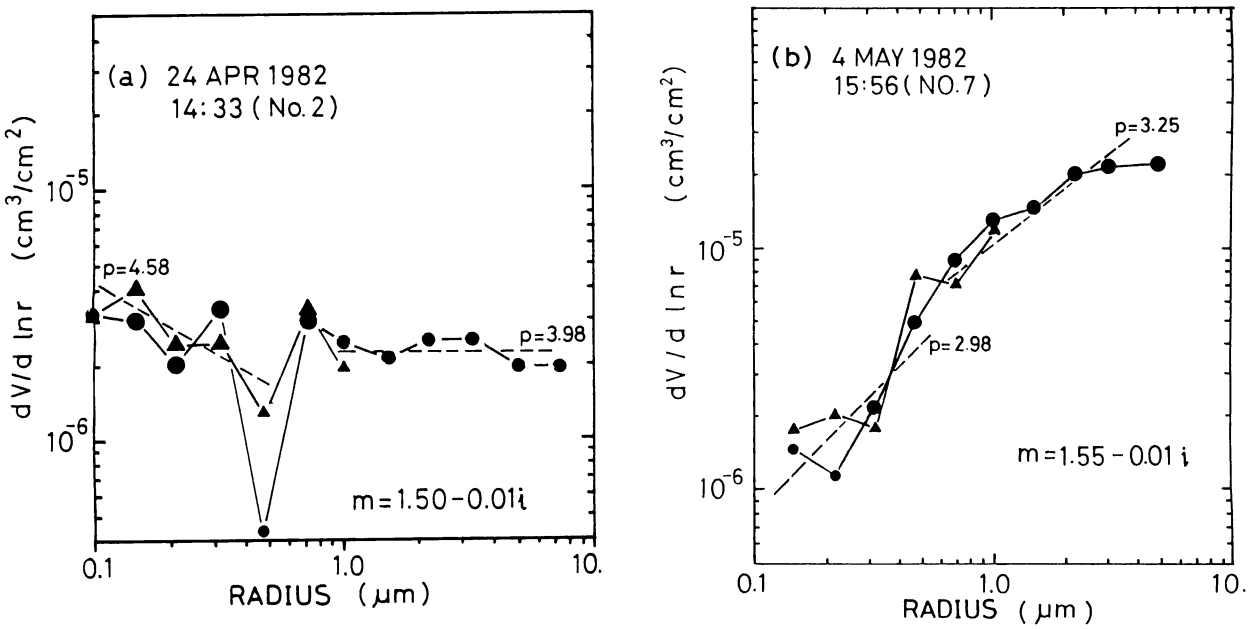

Fig. 8. Volume spectra of column aerosols retrieved from the data in Fig. 6. Circles and triangles correspond to inversions of the phase function plus optical thicknesses and the optical thickness only, respectively. Broken lines indicate p-values estimated from the optical thickness and the phase function for small and large particles, respectively : (a) 24 April 1982; (b) 4 May 1982.

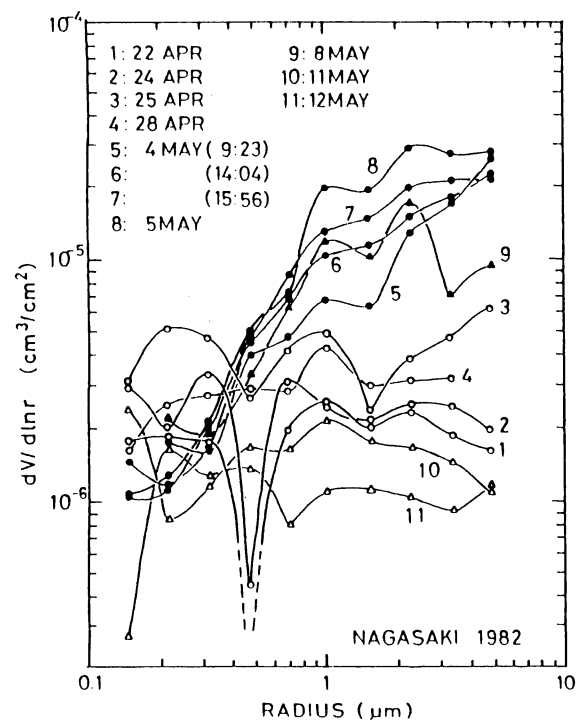

Fig. 9. Volume spectra for the whole observation period. Open and closed symbols correspond to the normal conditions and the yellow sand events, respectively.

Figure 9 shows the volume spectra retrieved in the observation period. The assumed refractive index of aerosols is $1.50 - 0.01i$ for the pre- and post-event stages and $1.55 - 0.01i$ for the yellow sand events independently of the wavelength. According to Carlson and Benjamin (1980), significant dependence of the absorption index on the wavelength was observed for Saharan dust particles due to selective absorption by various iron oxides such as hematite, limonite and magnetite (Kondratyev *et al.*, 1974; Ackerman and Toon, 1981). In spite of these facts, we assumed a gray refractive index because of the insensitivity of the forward scattering to the refractive index and of the uncertainty in the value of the absorption index of yellow sand particles. Essential features of the volume spectrum will be unchanged even if we include the wavelength dependence of the refractive index. From Fig. 9, it is found that the volume spectra in the pre- and post-event stages were multimodal or nearly Junge size distributions (spectra 1–4 and 10–11). The spectrum 5 in the first yellow sand event of 4 May had a significant portion of large particles indicating that the frontal air mass transported large particles before falling out. This volume spectrum can be approximated by a power law volume spectrum of $dV/d\ln r \sim Cr$. As time evolved, the spectra were modified; particles with radii around 2 μm largely increased while larger particles did not so increase (spectra 6–8). This would be interpreted by the fact that the air mass on a slow atmospheric flow arrived later and large particles tended to fall out during transportation. This interpretation is supported by the spectrum 9 of 8 May, in which large particles were ob-

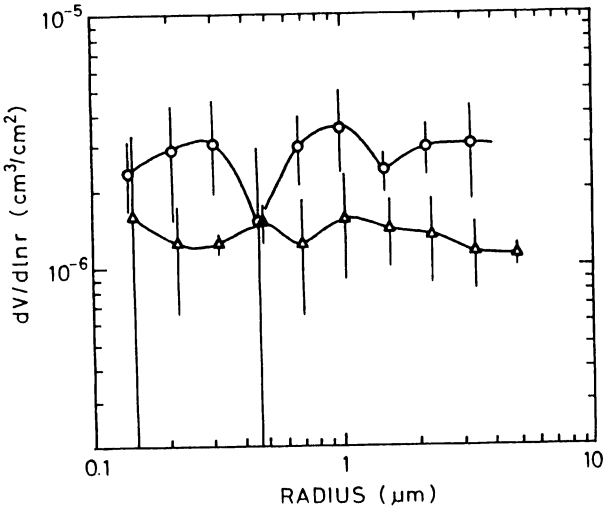

Fig. 10. Time averaged volume spectra for the pre-event (circles) and the post-event (triangles) stages of the yellow sand events. Vertical lines indicate standard deviations of the data.

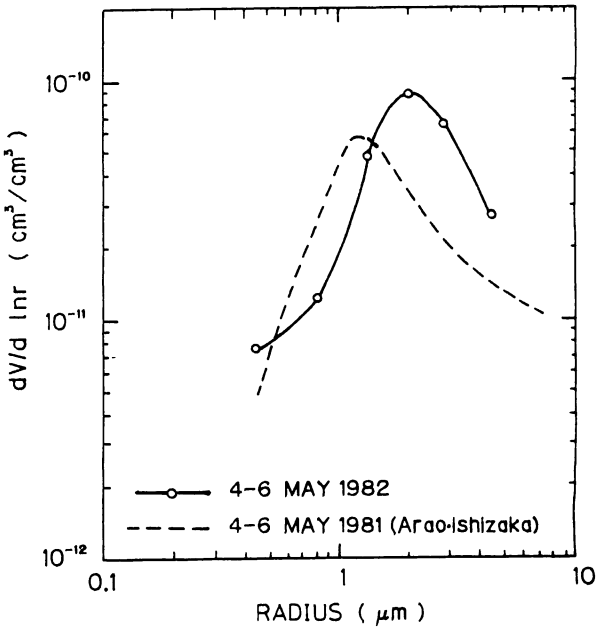

Fig. 11. Volume spectra of near-ground aerosols measured with the Andersen sampler in the period 4–6 May, 1982 (solid line with circles) by the authors and in the period 4–6 May, 1981 (broken line) by Arao and Ishizaka (1986).

viously eroded. Since the moving speed of the air mass for the second yellow sand event of 8 May was lower than the first event of 4–5 May as shown by the trajectories in Figs. 2 and 3, the fraction of lost particles in the second event was larger than that in the preceding one.

Another interesting feature in Fig. 9 is that small particles decreased in the yellow sand events as compared with the pre-event stage in spite of a significant increase of large particles. This tendency is consistent with the result of OPC as shown in Fig. 5. Though relative sensitivity of the inversion for small particles decreases due to significant contribution of large particles, the following reason would be a part of the cause of the phenomenon: the volume loading of aerosols in the continental air mass is generally smaller than that in an urban area of Japan. The air mass of the observation site of urban type was replaced with the continental origin air mass during the yellow sand events. Therefore it is not always adequate to estimate the loading of yellow sand particles by subtracting the optical thickness in the normal conditions from that in the event. Such a practice will underestimate the volume loading of yellow sand particles. From Fig. 5, it is roughly estimated that the number density of particles with radii between 0.15 and 0.25 μm was about 100/cm^3 in the normal conditions at Nagasaki, and was about 20/cm^3 in the continental air mass, and was as low as 10/cm^3 in the clean air mass associated with the frontal activity.

In Fig. 10 are shown the averaged volume spectra in the pre- and post-event periods. The long-term average tended to be the Junge size distribution, though each volume spectrum fluctuated showing multimodal shape as in Fig. 9. In Fig. 11 we show the volume spectrum obtained by the Andersen sampler assuming the density of the yellow sand particles to be 2.6 g/cm^3 (solid line). The volume spectrum had a sharp peak around 2 μm radius. The spectrum was somewhat different from the column volume spectra obtained by the aureolemeter, while it had a similar shape to that reported by Arao and Ishizaka (1986) (broken line). The most likely reason for this discrepancy is attributed to the large difference between the sampling times of the aureolemeter and Andersen sampler, as well as some difference in collection efficiency of the sampler among different sampling stages. We must also pay attention to the large inhomogeneity of the optical stratification of the yellow sand particles; the result of the Andersen sampler represents the feature just near the ground surface while that of the aureolemeter the total column average. The scale height defined by the ratio of the aerosol optical thickness to the extinction cross section estimated from the polar nephelometer measurement was as large as 4 km in the yellow sand events, which is somewhat larger than the main transporting altitude from map analyses. It means that the upper atmosphere was optically dense as compared with the near-ground atmosphere in the events.

5. Concluding remarks

Using the data obtained from several instruments, we have compared the optical characteristics of aerosols between in the normal atmospheric conditions and in yellow sand events.

In the normal conditions, an urban type air mass with a large fraction of sulfur and a small fraction of chlorine prevailed at the observation site as shown in Fig. 4. The optical thickness of aerosols at $\lambda = 0.5\mu$m varied from 0.2 to 0.8. The optical thickness and the Ångström's exponent α were strongly related to the humidity showing the predominance of hygroscopic aerosols. Averaged volume spectra retrieved from the aureolemeter data had a nearly Junge-type distribution, although each spectrum showed a multimodal distribution. The time evolution of the scattering cross section and the number density of aerosols closely related to that of the surface pressure indicating that the atmospheric turbidity at the observation site was controlled by the replacement of air mass and/or the rain-out effect associated with the frontal activity and the weather change.

From Figs. 4, 5 and 7, we found that the atmosphere of the observation site was affected significantly by the yellow sand particles in the period of 4–8 May 1982. The volume spectra retrieved from the aureolemeter and Andersen sampler showed the dominance of large particles with micron-order radii both for the total column and the near-ground air during the yellow sand events. As for the mode radius, however, there was some difference between the results obtained from those two measurements. The former showed a greater abundance of larger particles than the latter. This discrepancy is partly attributed to the fact that the volume spectrum obtained from the Andersen sampler is the time average for the period from beginning to end of the mature event including both weakened and enhanced stages, and partly to the vertical inhomogeneity in particle stratification.

Associated with the yellow sand events, it was found that an air mass exchange between the continental and the maritime took place. This was indicated by changes of the air humidity, the wind direction, the particle number density and the volume spectra as shown in Figs. 1, 5 and 9. The volume spectra retrieved from aureolemeter measurements and the number density measured by OPC showed apparently that the background submicron aerosols decreased in the yellow sand events by prevalence of the continental air mass. The optical thickness of aerosols at $\lambda = 0.5\mu$m was about 0.5–1.0 while the Ångström's exponent α was about 0.1–0.5. Since the loading of background aerosols is different between continental and urban (or maritime) air masses, a simple subtraction of the optical thickness in the normal conditions from that of yellow sand events will underestimate the column volume of yellow sand particles.

The analyses of synoptic phenomena and air mass trajectories supported the intrusion of a strong yellow sand storm on 4 May and a weak one on 8 May, which were generated in the arid region around the middle course of the Yellow River. However, we accept that the isobaric trajectory analysis employed in this paper is insufficient to discuss precisely the origin and the altitude of transportation. Since the wind speed was different among different levels in the atmosphere wherefrom the yellow sand particles falled out with different speeds depending on particle sizes, the column size distribution of the yellow sand particles might change in a complex fachion in time and space during their transportation. The size distribution of yellow sand particles and its temporal change reported in this paper will provide helpful information to elucidate such complex behavior, when it will be combined with a numerical simulation of particle transportation such as Kai *et al.* (1988) but taking account of the effect of gravitational sedimentation.

Although no event was recorded by Nagasaki Marine Observatory on 8 May, such potential contamination by yellow sand particles was also suggested by a large depolarization ratio in lidar signals (Kobayashi *et al.*, 1985). Thus, even if no event is apparently observed, it should be expected that a large amount of aerosol particles transported from the Chinese Continent occasionally prevails in the troposphere over Japan.

Acknowledgements.

The authors would like to appreciate the experimental support of the PIXE analysis of Prof. K. Kotajima of the Department of Nuclear Engineering and Prof. K. Ishii of the Cyclotron Radioisotope Center, Tohoku University. Drs. R. S. Fraser and Y. J. Kaufman of Goddard Space Flight Center and Dr. P. Koepke of the Munich University are gratefully acknowledged for valuable discussion. Thanks are also extended to Messrs. H. Imamura and Y. Miyazaki for their assistance of the measurements and to anonymous referees for their proper comments on this paper.

References

Ackerman, T.P. and O.B. Toon, 1981: Absorption of visible radiation in atmosphere containing mixtures of absorbing and nonabsorbing particles. *Appl. Opt.*, **20**, 3661–3668.

Ångström, A., 1964: The parameters of atmospheric turbidity. *Tellus*, **16**, 64–75.

Arao, K., Y. Makino and Y. Nagaki, 1979: Some statistical aspects of yellow sand. *Sci. Bull. Fac. Educ.*, Nagasaki Univ., **30**, 65–74 (in Japanese).

Arao, K. and Y. Ishizaka, 1986: Volume and mass of yellow sand dust in the air over Japan as estimated from atmospheric turbidity. *J. Meteor. Soc. Japan,* **64,** 79–94.

Asano, S. and M. Sato, 1980: Light scattering by randomly oriented spheroidal particles. *Appl. Opt.,* **19,** 962–974.

Braaten, D.A. and T.A. Cahill, 1986: Size and composition of Asian dust transported to Hawaii. *Atmos. Environ.,* **20,** 1105–1109.

Carlson, T.N. and S.G. Benjamin, 1980: Radiative heating rates for Saharan dust. *J. Atmos. Sci.* **37,** 193–213.

Carlson, T.N. and R.S. Caverly, 1977: Radiative characteristics of Saharan dust at solar wavelengths. *J. Geophys. Res.,* **82,** 3141–3152.

Darzi, M. and J.W. Winchester, 1982: Aerosol characteristics at Mauna Loa Observatory, Hawaii after East Asian dust storm episodes. *J. Geophys. Res.,* **87,** 1251–1258.

Duce, R.A., C.K. Unni, B.J. Ray, J.M. Prospero and J.T. Merrill, 1980: Long-range atmospheric transport of soil dust from Asia to the tropical North Pacific: Temporal variability. *Science,* **209,** 1522–1524.

Iwasaka, Y., H. Minoura, K. Nagaya and A. Ono, 1982: The transportation and spacial scale of dust storm, KOSA.— A case study on the dust storm of April 1979 measured by lidar. *Tenki,* **29,** 231–235 (in Japanese).

Junge, C.E., 1979: The importance of mineral dust as an atmospheric constituent. *Saharan Dust,* C. Morales, Ed., Wiley, 49–60.

Kadowaki, S., 1979: Silicon and aluminum in urban aerosols for characterization of atmospheric soil particles in the Nagoya area. *Environ. Sci. and Tech.,* **13,** 1130–1133.

Kai, K., Y. Okada, O. Uchino, I. Tabata, H. Nakamura, T. Takagi and Y. Nikaidou, 1988: Lidar observation and numerical simulation of a Kosa (Asian dust) over Tsukuba, Japan during the spring of 1986. *J. Meteor. Soc. Japan,* **66,** 457–472.

Kaufman, Y.J. and R.S. Fraser, 1983: Light extinction by aerosols during summer air pollution. *J. Clim. and Appl. Meteor.,* **22,** 1694–1706.

Kobayashi, A., S. Hayashida, K. Okada, and Y. Iwasaka, 1985: Measurements of the polarization properties of Kosa (Asian dust-storm) particles by a laser radar in spring 1983. *J. Meteor. Soc. Japan,* **63,** 144–149.

Kondratyev, K. Ya, O.B. Vassilyev, V.S. Grishechkin and L. S. Ivlev, 1974: Spectral radiative flux divergence and its variability in the troposphere in the 0.4–2.5 m., *Appl. Opt.,* **13,** 478–486.

Kondratyev, K. Ya, R.M. Welch, S.K. Cox, V.S. Grishechkin, V.A. Ivanov, M.A. Prokofyev, V.F. Zhvalev and O.B. Vasilyev, 1981: Determination of vertical profiles of aerosol size spectra from aircraft radiative flux measurements. 1. Retrieval of spherical particle size distribution. *J. Geophys. Res.,* **86,** 9783–9793.

Nakajima, T., M. Tanaka and T. Yamauchi, 1983: Retrieval of the optical properties of aerosols from aureole and extinction data. *Appl. Opt.,* **22,** 2951–2959.

Nakajima, T., T. Takamura, M. Yamano, M. Shiobara, T. Yamauchi, R. Goto and K. Murai, 1986: Consistency of aerosol size distributions inferred from measurements of solar radiation and aerosols. *J. Meteor. Soc. Japan,* **64,** 765–776.

Nakajima, T., M. Tanaka, M. Yamano, M. Shiobara, K. Arao and Y. Nakanishi, 1989: Aerosol optical characteristics in the yellow sand events observed in May, 1982 at Nagasaki - Part II Models., *J. Meteor. Soc. Japan.,* **67,** 279–291.

Prodi, F. and C. Tomasi, 1983: Sahara dust program-I. The Italian network of sun-photometers. Extinction models based on multimodal particle size distributions. *J. Aerosol. Sci.,* **14,** 517–527.

Shaw, G.E., 1977: Physical and climatic properties of the global aerosol. *Radiation in the atmosphere.* H.-J. Bolle, Ed., Science Press, 472–474.

Shaw, G.E., 1980: Transport of Asian desert aerosol to the Hawaiian Islands. *J. Appl. Meteor.,* **19,** 1254–1259.

Takamura, T., M. Tanaka and T. Nakajima, 1984: Effects of atmospheric humidity on the refractive index and the size distribution of aerosols as estimated from light scattering measurements. *J. Meteor. Soc. Japan,* **62,** 573–582.

Takayama, Y. and T. Takashima, 1986: Aerosol optical thickness of yellow sand over the yellow sea derived from NOAA satellite data. *Atmos. Environ.,* **20,** 631–638.

Takeda, T., P.-M. Wu and K. Okada, 1986: Dependence of light scattering coefficient of aerosols on relative humidity in the atmosphere of Nagoya. *J. Meteor. Soc. Japan,* **64,** 957–966.

Tanaka, M., T. Nakajima and T. Takamura, 1982: Simultaneous determination of complex refractive index and size distribution of airborne and water-suspended particles from light scattering meas urements. *J. Meteor. Soc. Japan,* **60,** 1259–1272.

Tanaka, M., T. Nakajima and M. Shiobara, 1986: Calibration of a sunphotometer by simultaneous measurements of direct-solar and circumsolar radiations. *Appl. Opt.,* **25,** 1170–1176.

Tanaka, M., T. Takamura and T. Nakajima, 1983a: Refractive index and size distribution of aerosols as estimated from light scattering measurements. *J. Clim. Appl. Meteor.,* **22,** 1254–1261.

Tanaka, S., S. Tamura, Y. Hashimoto and T. Otoshi, 1983b: Long range transportation of soil dust from Asian continent to Japan and its influence to the atmosphere in Japan - by the results of NASN (National Air Survey Network) data. *J. Japan Soc. Air Pollut.,* **18,** 263–270.

Tomasi, C., F. Prodi and F. Tampieri, 1979: Atmospheric turbidity variations caused by layers of Sahara dust particles. *Contr. Atmos. Phys.,* **52,** 215–228.

Welch, R.M., S.K. Cox and K.Ya. Kondratyev, 1981: Determination of vertical profiles of aerosol size spectra from aircraft radiative flux measurements 2. The effect of particle nonsphericity., *J. Geophys. Res.,* **86,** 9795–9800.

Winchester, J.W., L. WeiXiu, R. LiXin, W. MingXing and W. Maenhaut, 1981: Fine and coarse aerosol composition from a rural area in North China. *Atmos. Environ.*, **15**, 933–937.

Yamamoto, G. and M. Tanaka, 1969: Determination of aerosol size distribution from spectral extinction measurements. *Appl. Opt.*, **8**, 447–453.

長崎における1982年5月の黄砂の光学特性

第1部　観測

田中正之・塩原匡貴[1]・中島映至・山野牧[2]

（東北大学理学部超高層物理学研究施設）

荒生公雄

（長崎大学教育学部地学教室）

1982年5月4日から8日にかけて長崎市において観測された黄砂現象について、太陽直達光と太陽周辺光の分光観測からエアロゾルの光学的厚さと粒径分布（体積スペクトル）を求めた。その結果、半径数ミクロンの大粒子の増大とサブミクロン粒子の減少が見出された。オーリオールメータ観測から得られた黄砂の体積スペクトルのモード半径は2 μ mより大きかった。平時の波長0.5 μ mでのエアロゾルの光学的厚さが0.2～0.8、オングストローム指数 α が0.8～1.5であったのに対して、黄砂時には、各々0.5～1.0、0.1～0.5と大きく変化した。地上・高層天気図を用いた流跡線解析、およびエアゾルの元素分析、数密度、散乱断面積の観測結果は、黄砂の到来が前線の移動に伴う大陸気団の卓越によることを支持した。

[1]現在所属：気象研究所、茨城県つくば市長峰1-1

[2]現在所属：川崎市多摩区長尾2-9-10